Revista Brasileira de Entomologia 70(3):e20260035, 2026

SOCIEDADE BRASILEIRA DE ENTOMOLOGIA
FUNDADA EM 1937

REVISTA BRASILEIRA DE
Entomologia
A Journal on Insect Diversity and Evolution

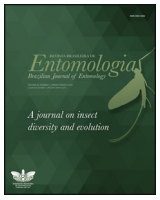

Redescription of the immature stages of *Angelabella tecomae* (Lepidoptera, Gracillariidae) with notes on mandibular morphology and leaf damage on *Tecoma fulva* (Bignoniaceae)

José Cerdeña[1]*, Jackie Farfán[2], Héctor A. Vargas[3], Gerardo Lamas[4]

[1]*Universidad Nacional Mayor de San Marcos, Facultad de Ciencias Biológicas, Programa de Doctorado en Ciencias Biológicas, Lima, Perú.*
[2]*Universidad Nacional de San Agustín de Arequipa, Museo de Historia Natural, Arequipa, Perú.*
[3]*Universidad de Tarapacá, Facultad de Ciencias Agronómicas, Departamento de Recursos Ambientales, Arica, Chile.*
[4]*Universidad Nacional Mayor de San Marcos, Museo de Historia Natural, Departamento de Entomología, Lima, Perú.*

ARTICLE INFO

Article history:
Received 20 April 2026
Accepted 17 June 2026
Available online 31 July 2026
Associate Editor: Karina Brandão

Keywords:
Oecophyllembiinae
Chaetotaxy
Ontogeny
Leaf-mining micromoths
Larval instars

ABSTRACT

Angelabella tecomae Vargas & Parra, 2005, is a leaf-mining micromoth inhabiting xerophytic environments along the western slopes of the Andes in northern Chile and southern Peru, where it is associated with plants of the genus *Tecoma* Jussieu. Its hypermetamorphic development includes two larval forms: a sap-feeding form during the first four instars, and a spinning form in the final instar. Recent evidence suggests the existence of cryptic diversity within *Angelabella* Vargas & Parra, 2005 across its geographic range, indicating that the genus may comprise several candidate species that remain unrecognized under current taxonomy. To contribute to the accurate identification of *A. tecomae*, we provide a detailed redescription of its immature stages based on current standards of descriptive morphology. The sap-feeding and spinning larvae, as well as the pupa, are described in detail using scanning electron microscopy images and illustrated with detailed chaetotaxal maps. In addition, histological sections of leaflets of *Tecoma fulva* (Cavanilles) D. Don (Bignoniaceae), were examined to characterize the leaf damage produced by the sap-feeding instars and to assess their ontogenetic relationship with changes in mandibular morphology.

Introduction

The morphology of immature stages in Lepidoptera is essential for understanding larval biology and provides taxonomically informative characters that complement adult morphology, particularly among cryptic species, in which larval or pupal traits enhance species discrimination (Friberg, 2007; Davis and Wagner, 2011; Álvarez et al., 2025; Garzón-Orduña and Brower, 2025). Larval morphology, especially mandibular structure, plays a key role in determining feeding behavior and the extent of foliar damage in leaf-mining Gracillariidae (Kumata, 1978; Body et al., 2015), which exhibit hypermetamorphic larval development, with early instars possessing flattened mandibles adapted for superficial sap-feeding restricted to epidermal or subepidermal tissues, whereas later instars develop normal chewing type mandibles capable of penetrating and consuming parenchymal tissues (Body et al., 2015; Pereira et al., 2019). These ontogenetic modifications not only influence larval ecology but also provide informative morphological characters for species diagnosis and differentiation in systematic studies (Kawahara et al., 2017). Despite the recognized importance of larval morphology, detailed descriptions of mouthparts and head structures based on high-resolution imaging remain scarce for many gracillariid species.

Oecophyllembiinae is one of three gracillariid subfamilies, along with Phyllocnistinae and Marmarinae, whose larvae lack tissue-feeding instars; instead, sap-feeding instars are followed by a non-feeding, highly specialized, spinning instar (Kawahara et al., 2017). Consequently, leaf mines are typically constructed only by the sap-feeding larva, which does not consume solid tissue particles but feeds by ingesting cellular fluids (Kumata, 1998). The subfamily currently includes six genera: *Angelabella* Vargas & Parra, 2005; *Corythoxestis* Meyrick, 1921; *Eumetriochroa* Kumata, 1998; *Guttigera* Diakonoff, 1955; *Metriochroa* Busck, 1900; and *Prophyllocnistis* Davis, 1994. Recent contributions within Oecophyllembiinae have improved knowledge of pupal morphology in several genera, such as *Corythoxestis*, *Eumetriochroa*, *Guttigera*, and *Metriochroa*, highlighting the taxonomic value of immature characters within the subfamily (Kobayashi et al., 2011, 2013). However, detailed larval and pupal morphological data for *Angelabella* have remained poorly documented since its original description (Vargas and Parra, 2005).

*Corresponding author.
E-mail: jose.cerdena@unmsm.edu.pe (J. Cerdeña).

https://doi.org/10.1590/1806-9665-RBENT-2026-0035

The genus *Angelabella* is currently represented by a single described species, *Angelabella tecomae* Vargas & Parra, 2005, a leaf-mining micromoth distributed along the western slopes of the Andes from central Peru to northern Chile. Its primary host plant is the shrub *Tecoma fulva* (Cavanilles) D. Don (Bignoniaceae). The original description of the genus and species included a characterization of the immature stages, comprising the pupa and two larval forms, which consist of four sap-feeding instars and a single spinning instar. However, these descriptions were based on a limited number of low-resolution microscopy images, which were insufficient for a detailed characterization of larval morphology and chaetotaxy (Vargas and Parra, 2005). Furthermore, recent evidence suggests the existence of cryptic diversity within *Angelabella* across its geographic range, indicating that this lineage may comprise multiple evolutionary units that remain undescribed (Vargas-Ortiz et al., 2020). Detailed morphological data from immature stages are therefore essential for resolving species boundaries and improving our understanding of evolutionary relationships within this group.

In this context, we provide a detailed redescription of larval and pupal morphology using high-resolution scanning electron microscopy (SEM), chaetotaxal maps, and histological analysis of larval foliar damage. By focusing on ontogenetic changes in mandibular morphology and their functional implications for feeding mode transitions, this study aims to improve diagnostic tools for species identification and to establish a baseline for future taxonomic, ecological, and evolutionary studies of *Angelabella* and related gracillariids.

Material and methods

Immature specimens used in this study were obtained from leaves with leaf-mining larvae, as well as from pupae collected on *Tecoma fulva*, at the type locality of *A. tecomae* (Azapa Valley, Arica, Chile) (Fig. 1). At least 10 specimens of each larval form and pupa were collected. The morphological terminology used herein follows the work of Davis (1987, 1994).

Immature stages were preserved in 95% ethanol. For descriptions of morphology, specimens were examined using a Leica® M125 stereomicroscope. Structures or shapes selected for illustration were first photographed with a digital camera mounted on the stereomicroscope. Line drawings were then produced using Adobe Photoshop, with the corresponding digital images serving as a guide. At least five specimens were examined for the description of each life stage or instar.

For scanning electron microscope (SEM) analyses, additional larval and pupal specimens were dehydrated using a Bal-tec® CPD030 critical-point dryer, mounted on metal stubs with double-sided adhesive tape, and sputter-coated with gold in a Bal-tec® SCD050 coater. The specimens were subsequently examined and photographed using a Thermo Scientific® QuattroS scanning electron microscope at the Museo de Historia Natural, Universidad Nacional Mayor de San Marcos de Lima, Perú (MUSM).

For the preparation of mandibles from sap-feeding larval instars, the mouthparts were carefully manipulated using a stylet made from an entomological pin (No. 2) attached to a metal handle. This procedure allowed the cephalic capsule to be opened, and the labrum and labium to be removed, thereby exposing the mandibles. The cephalic capsules were then processed following the SEM preparation protocol described above. For the determination of sap-feeding larval instars, head capsule width was measured, and instars were classified following the range of measurements described for *A. tecomae* by Storey-Palma et al. (2012).

Images of plant anatomy were based on diaphanized, field-collected leaf mines (n = 5) from *T. fulva* shoots. Samples were fixed in FAA (37% formaldehyde, glacial acetic acid, and 50% ethanol, 1:1:18, v/v), stained with safranine (aqueous solution: 100 mg/L), and mounted either whole or in freehand sections in glycerin on slides, following the procedure described in detail by Brito et al. (2012).

Results

Morphological description of the larva and pupa of Angelabella tecomae *Vargas & Parra 2005*

Larva. Leaf-miner, endophyllous, with hypermetamorphic development comprising five instars. The first four instars are sap-feeding, showing no stable differences in body shape or coloration among them, while the last instar is non-feeding, called the 'spinning' instar.

Sap-feeding instars (Figs. 1E, 2)

Body flattened dorsoventrally, yellowish-translucent (Fig. 1E). **Head**: Prognathous, brown, markedly depressed; stemmata absent. Labrum well developed, basal width approximately half of distal width; dorsal surface bearing a lobular comb over the distal half, anterior margin weakly invaginated at midline, with a pair of microsetae at the posterior base and two pairs of pores near the anterior margin of the frontoclypeus (Fig. 2D). Mandibles plate-like, subcircular, and dorsoventrally flattened; incisor region bearing two apical teeth, molar area flattened with a finely serrated mesial margin and a lateral pore near the base on the outer side. Labium slightly wider than labrum; hypopharyngeal spines extending to the base of the labium, posteriorly directed, postmentum bearing three pairs of setae (LB1, LB2, LB3). Maxillary and labial palpi absent. Antennae unsegmented, laterally and subapically positioned immediately posterior to the mouthparts; length approximately two-thirds that of the labrum; with four apical digitiform antennal lobes, three well developed and a fourth markedly reduced, and a lateral seta present (Fig. 2F). **Thorax**: Thoracic segments apodous. Prothoracic dorsal and ventral shields light brown; integument bearing numerous small setiform spinules of variable length (Fig. 2K), modified into scale-like structures along the proximal margin of the dorsal shield, one pair of pores present on middle of dorsal shield. Spiracles present on T2 (Fig. 2H, I). **Abdomen**: Integument of abdominal segments bearing numerous small setiform spinules of variable length (Fig. 2M). Segments A3–A6 with ambulatory callosities (Fig. 2L); segment A9 with pleural lobes positioned lateroventrally, each bearing a spiniform projection (Fig. 2O). Spiracles present on A1–A8.

Chaetotaxy of the fourth sap-feeding instar (Fig. 3)

Head: Nine pairs of setae are present on the head of the sap-feeding instar (excluding mouthparts), distributed as follows: in the laterodorsal region (relative to the antennal position), from anterior to posterior: A1, P1, and P2; in the lateral region: S1, S2, and L1; and in the lateroventral region: SS1, SS2, and S3. Setae A1, SS1, and S1 are distinctly longer than the remaining setae.

Body chaetotaxy: *Prothorax (T1).* XD group bisetose; XD1 and XD2 nearly equal in length, located on the prothoracic shield. D group unisetose; D1 situated posterodorsally on the prothoracic shield. SD group bisetose; SD1 longer than and anterodorsal to SD2. L group bisetose; L1 and L2 longer than and anterodorsal to SV1. SV group trisetose; SV1 longer than and posterodorsal to SV2 and SV3. V group unisetose; V1 arising from the middle of the ventral shield and positioned anteroventral to SV3.

Meso- (T2) and metathorax (T3). D group bisetose; D1 located in the posterodorsal region of the segment and to D2. SD group unisetose;-SD1 longer than and anterodorsal to L2. L group bisetose; L1 longer than and anteroventral to L2. SV group bisetose; SV1 posterodorsal to SV2. V group unisetose; V1 arising from the middle of the ventral surface and positioned anteroventral to SV2.

A1-8: D group bisetose; D1 longer than and posterodorsal to D2. SD group unisetose (SD1). L group unisetose; L1 and SD1 subequal in length and the longest setae on the segment. SV group bisetose; SV1 anterodorsal to SV2, SV2 absent on A7 and A8 segments. V group unisetose; V1 arising from the middle of the ventral surface.

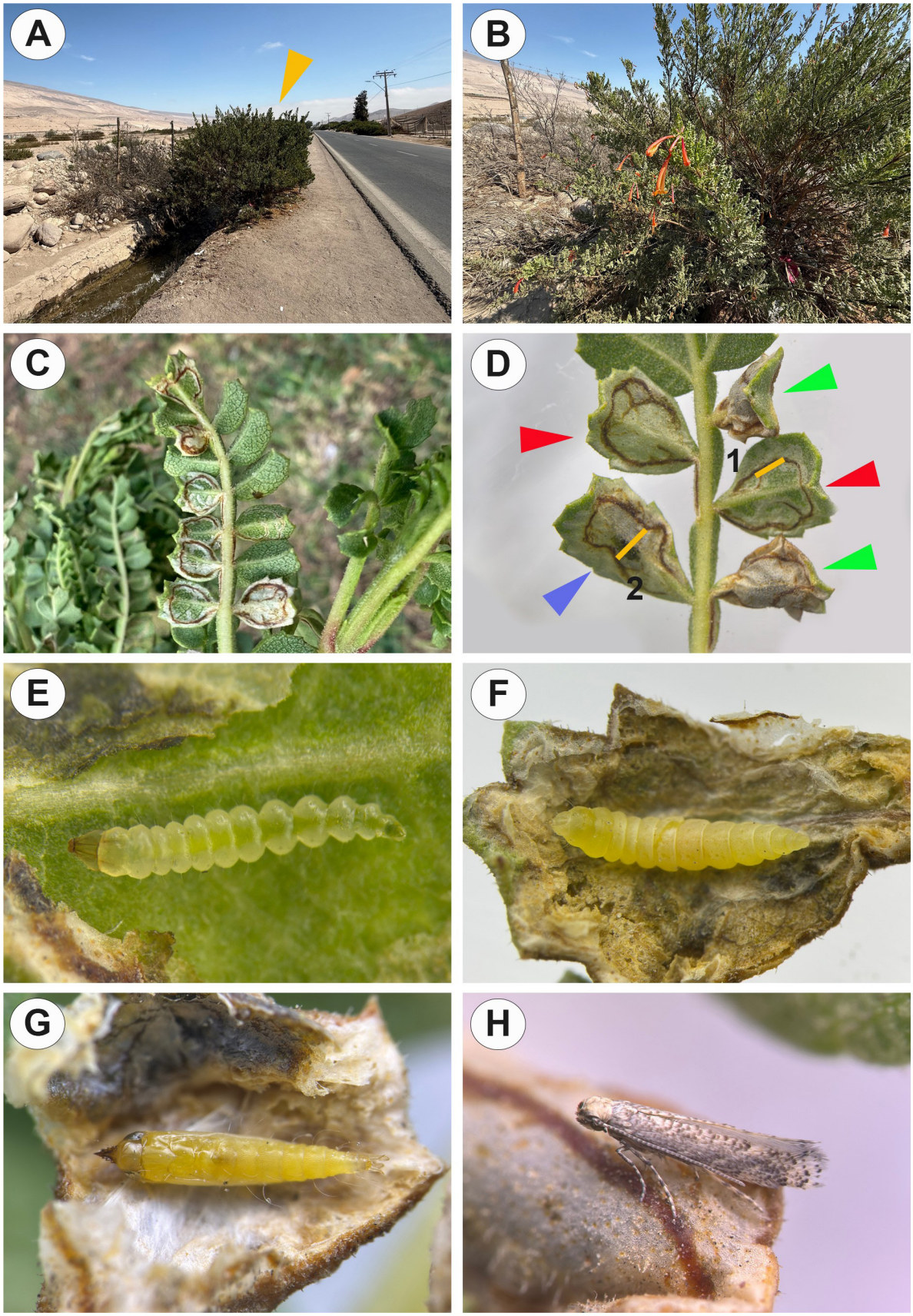

Figure 1 Natural history of *A. tecomae*. In: (A) type locality in Azapa Valley, Arica, Chile (*Tecoma fulva* host plant pointed by arrow head); (B) *Tecoma fulva* shrub under close view; (C) leaves of *T. fulva* with leaf-mining larvae of *A. tecomae* on abaxial surfaces; (D) leaflets of *T. fulva* with different immature stages of *A. tecomae* on abaxial surfaces (third sap-feeding instar pointed by red arrow heads, initial fourth sap-feeding instar pointed by blue arrow head, pupal chamber pointed by green arrow heads, numbers indicate position of histological sections presented in Fig. 7); (E) sap-feeding larva, dorsal; (F) spinning larva, dorsal view; (G) pupa, dorsal; (H) adult in resting posture

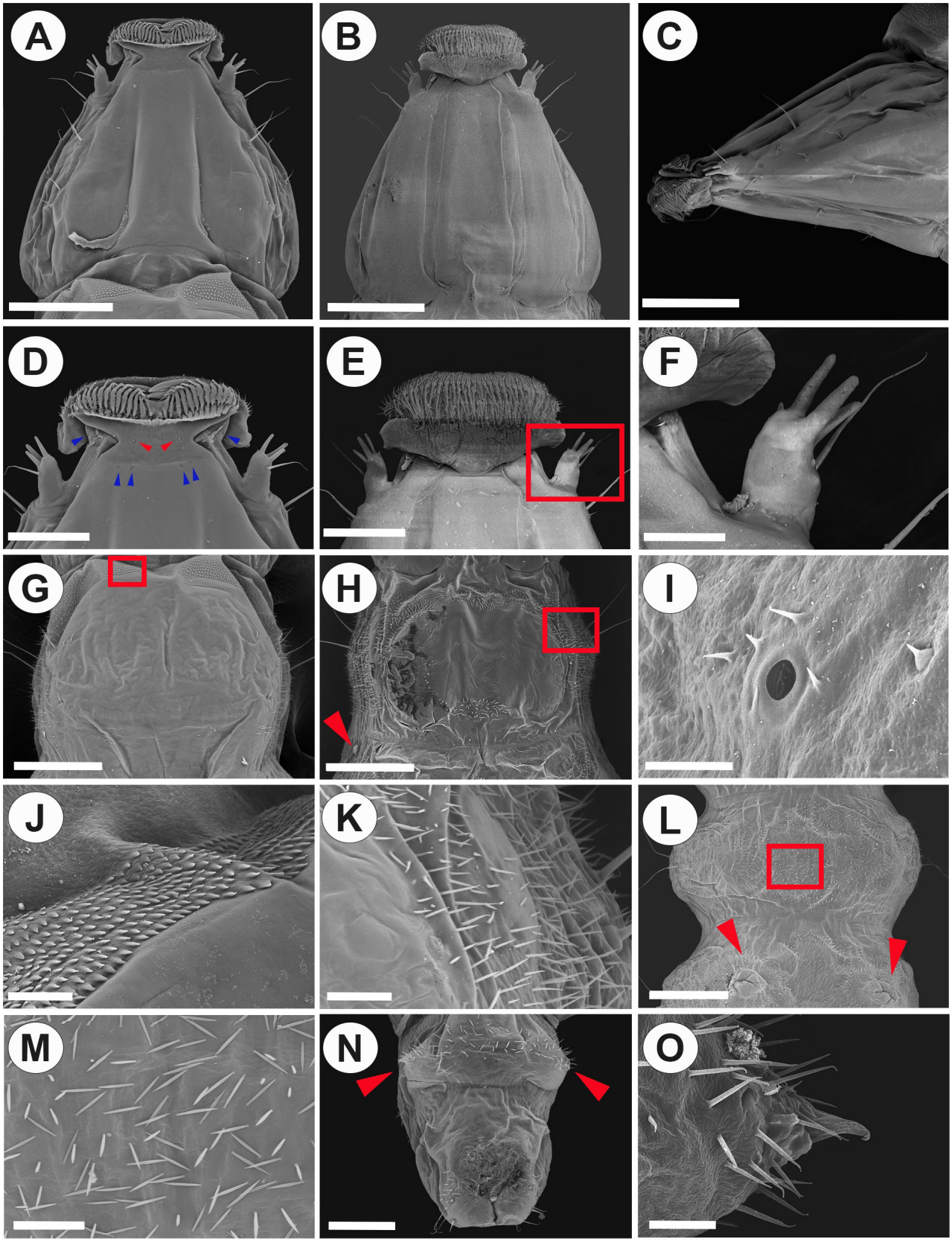

Figure 2 Scanning electron micrographs of *A. tecomae* sap-feeding larva (fourth instar). In: (A) head, dorsal view; (B) head, ventral view; (C) head, lateral view; (D) labrum, dorsal view (microsetae pointed by red arrow heads, pores pointed by blue arrow heads); (E) labium, ventral view; (F) antenna (indicated by square in E); (G) prothoracic dorsal shield; (H) prothoracic ventral shield; (I) thoracic spiracle (pointed by red arrow head in H); (J) proximal margin of the prothoracic dorsal shield (indicated by square in G); (K) setiform spinules of prothoracic ventral shield (indicated by square in H); (L) abdominal segments A2 and A3 (ambulatory callosities pointed by red arrow heads); (M) setiform spinules of abdominal segment A2 (indicated by square in L); (N) abdominal segments A9 and A10, ventral; (O) pleural lobe in A9 segment (pointed by red arrow heads in N). Scale bars: 100 µm (A, B, C, G, H, N); 50 µm (D, E); 15 µm (F, J, K, O); 10 µm (I); 150 µm (L); 20 µm (M)

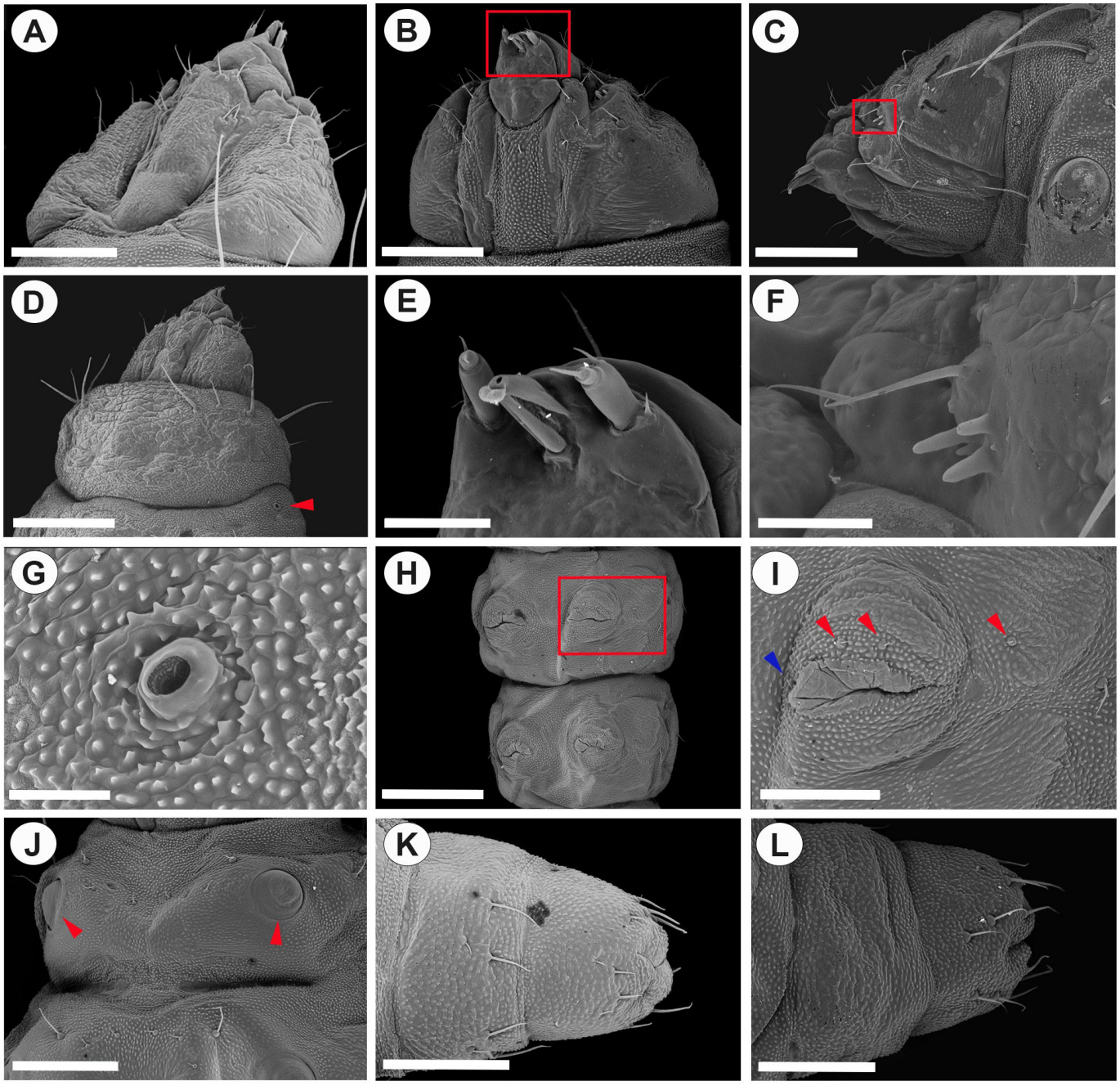

Figure 3 Head and body chaetotaxy of sap-feeding larva of *A. tecomae*. In: (A) head, dorsal view; (B) head, ventral view; (C) thoracic (T1 – T3) and abdominal segments (A1 – A10)

A9: SV group unisetose; SV1 anteroventral to pleural lobe.

A10: D group bisetose; D1 anterodorsal to D2. SD group bisetose; SD1 anterodorsal to SD2. L group unisetose; L1 shorter than D and SD setae and positioned posteroventral to SD2. SV group unisetose; SV1 anteroventral to L1. Ventral group unisetose (V1).

Spinning instar (Figs. 1F, 4)

Body cylindrical, with yellowish coloration (Fig. 1F). **Head**: Sub-spherical. Anterior lobe conspicuous, bearing a spinneret and well-differentiated labial palps in a subapical, ventral position. Frontoclypeus elongate-quadrangular. Stemmata absent. Labrum short, transversal, slightly bilobed apically, with three pairs of setae arranged in a transverse line near the apical margin. Mandibles dorsoventrally flattened, rudimentary, with three obtuse teeth and one pair of setae on the outer surface. Spinneret subconical, with a lobular apex; silk outlet opening located subterminally (Fig. 4E). Labial palps subcylindrical, three-segmented, approximately three-quarters the length of the spinneret. Basal segment conspicuously longer than the apical one and bearing a subterminal seta. Maxillary palps slender, bearing four pairs of setae: one pair in the apical area, one in the medial area, and two pairs at the base. Prementum with one pair of setae near the labial margin. Antennae unsegmented; with four apical digitiform antennal lobes, three well developed and a fourth markedly reduced, and a lateral seta present (Fig. 4F). **Thorax and abdomen**: Integument covered with numerous small tuberculiform spinules, irregularly distributed. Thoracic segments with circular pedal vestiges (Fig. 4J). Ambulatory callosities ("prolegs reduced") present on abdominal segments A3–A6 (Fig. 4I). Spiracles present on T2 and A1–A8 (Fig. 4G).

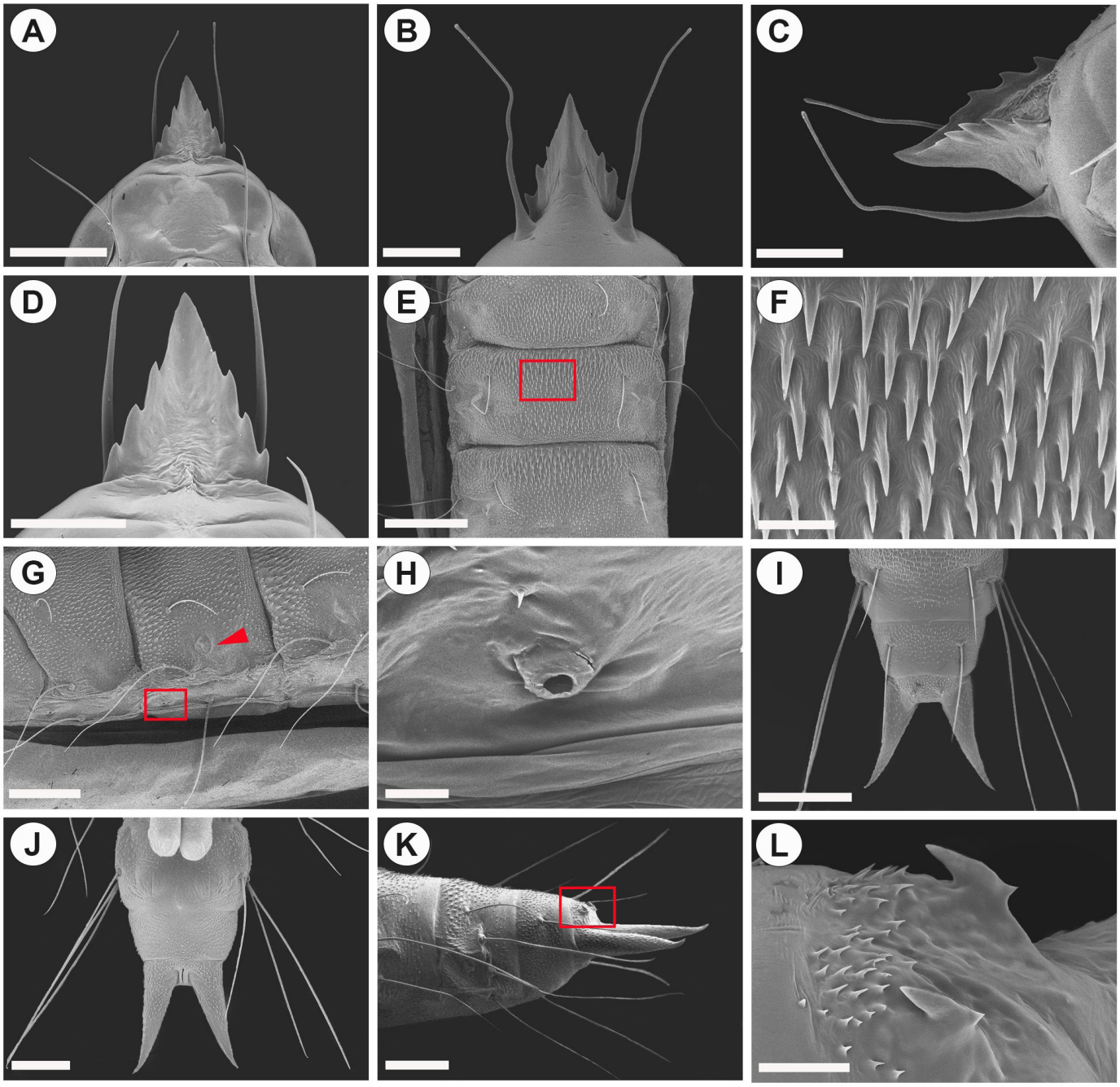

Figure 4 Scanning electron micrographs of *A. tecomae* spinning larva. In: (A) head, dorsal view; (B) head, ventral view; (C) head, lateroventral view; (D) prothoracic segment and head, dorsal view (mesothoracic spiracle pointed by red arrow head); (E) spinneret and labial palps, ventral view (indicated by square in B); (F) antenna, lateral view (indicated by square in C); (G) mesothoracic spiracle in detail (pointed by red arrow head in D); (H) abdominal segments A5 and A6, ventral view; (I) abdominal ambulatory callus in detail (indicated by square in H, SV group setae pointed by red arrow heads, D1 seta pointed by blue arrow head); (J) prothoracic and mesothoracic segments, ventral view (circular pedal vestiges pointed by red arrow heads); (K) abdominal segments A9 and A10, dorsal view; (L) abdominal segments A9 and A10, ventral view. Scale bars: 100 µm (A, B, C, I, J, K, L); 200 µm (D); 25 µm (E, F); 15 µm (G); 300 µm (H)

Chaetotaxy of spinning instar (Fig. 5)

Head: Twelve pairs of setae are present on the head (excluding mouthparts), distributed as follows: frontoclypeal area bearing C1 and C2; in the laterodorsal region (relative to the antennal position), from anterior to posterior: A1, P1, P2, MD1, and MD2; in the lateral region: S1, S2, and S3; and in the lateroventral region: SS1 and SS2. Setae A1, SS1, and S1 are longer than the remaining setae.

Body chaetotaxy: *Prothorax (T1).* XD group bisetose; setae nearly equal in length, XD1 in anterodorsal position to XD2. D group unisetose; D1 shorter than and posterodorsal to XD1. SD group bisetose; SD1 anterodorsal to SD2. L group bisetose; setae nearly equal in length, L1 posteroventral to L2. SV group trisetose; SV1 and SV2 nearly equal in length, SV3 anterodorsal to V1. V group unisetose (V1).

Meso- (T2) and metathorax (T3). D group bisetose; setae nearly equal in length, D1 posterodorsal to D2. SD group unisetose; SD1 longer than and posteroventral to D2. L group bisetose; setae nearly equal in length. SV group trisetose; SV1 longer than and posterodorsal to SV2, SV3 closer to V1. V group unisetose; V1 nearly equal in length than SV3.

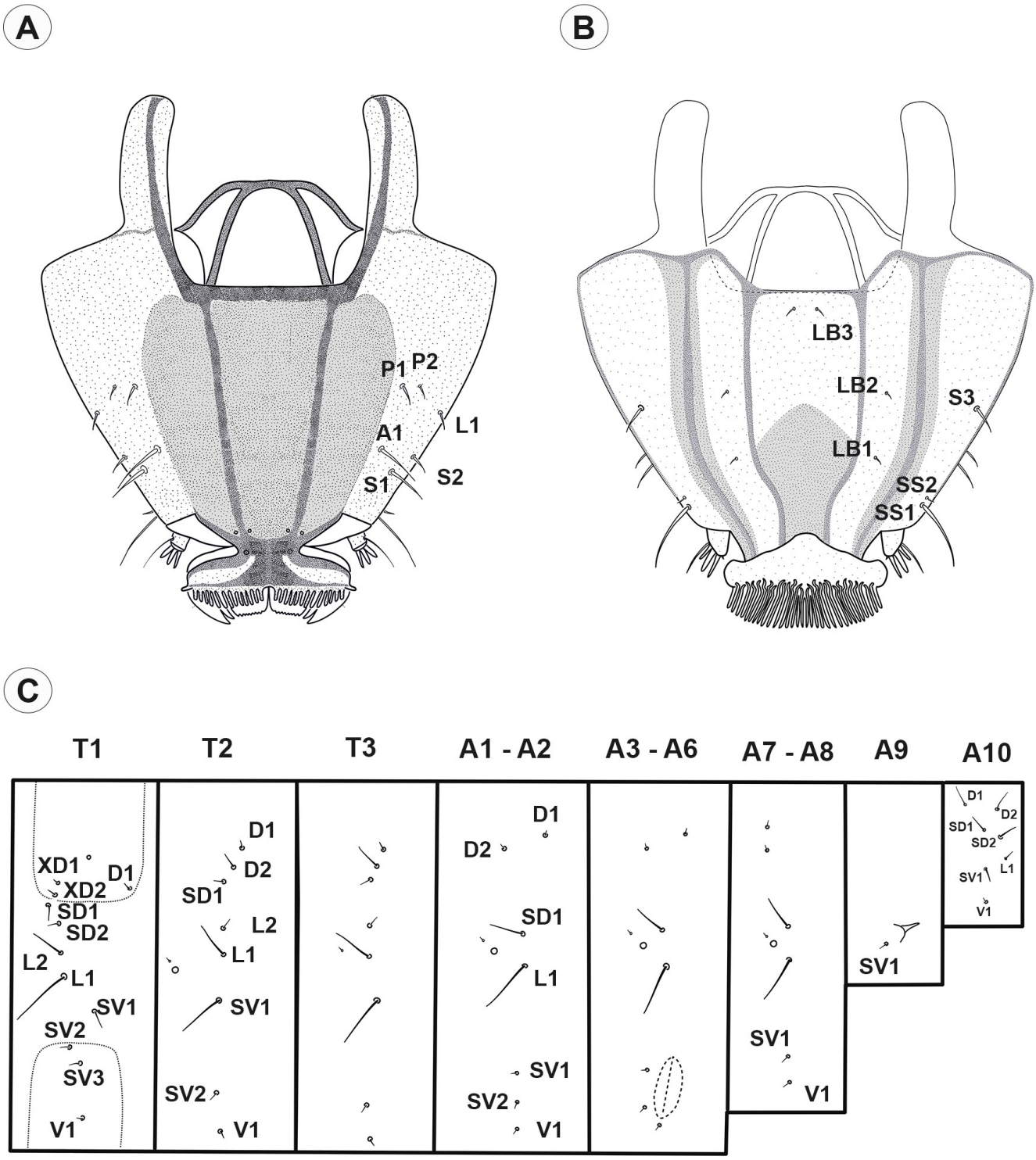

Figure 5 Head and body chaetotaxy of spinning larva of *A. tecomae*. In: (A) head, dorsal view; (B) head, ventral view; (C) thoracic (T1 – T3) and abdominal segments (A1 – A10), arrow pointed in SV2 seta, absent in A1

A1-8: D group bisetose; D1 posterodorsal to D2. SD group unisetose; SD1 posterodorsal to stemmata. L group unisetose (L1). SV group unisetose in A1, A7, and A8 (SV1), bisetose in A2 (SV1, SV2), and trisetose in A3–A6 (SV1, SV2, SV3); V group unisetose (V1).

A9: D group bisetose; D2 longer than and posterodorsal to D1. SD group unisetose (SD1).

A10: Terminal segment with eight pairs of setae (D1, D2, SD1, L1, L2, SV1, SV2, and V1).

Pupa (Figs. 1G, 6)

Yellowish, with the apex of the head dark brown (Fig. 1G). A sharp subpyramidal process with serrate lateral margins is present at the cephalic apex (Fig. 6D), with a pair of long, filiform setae inserted near its base (Fig. 6B). Antennal apices extending beyond the abdominal end. Apices of the proboscis and prothoracic legs coincident. Wing apices extending beyond those of the mesothoracic legs but not reaching the distal margin of abdominal segment A5.

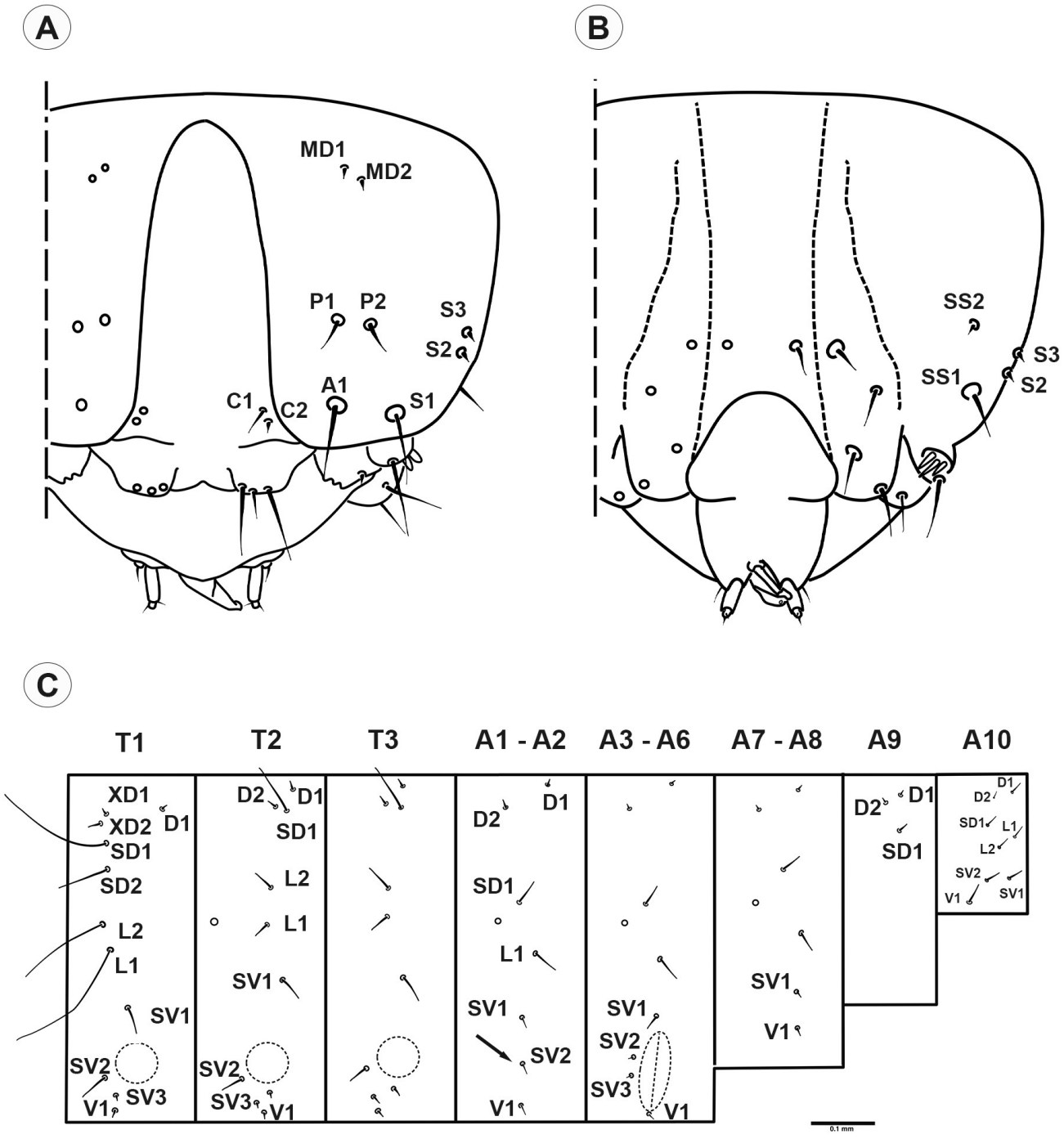

Figure 6 Scanning electron micrographs of *A. tecomae* pupa. In: (A) head, dorsal view; (B) cephalic process, ventral view; (C) cephalic process, lateral view; (D) cephalic process in detail, dorsal view; (E) abdominal segments A1-A3, dorsal view; (F) abdominal tergal spines in detail (indicated by square in E); (G) abdominal segments A1-A3, lateral view ("lateral callosity" pointed by red arrow head); (H) abdominal spiracle in detail (indicated by square in G); (I) last abdominal segments A8-A10, dorsal view; (J) last abdominal segments A8-A10, ventral view; (K) last abdominal segments A8-A10, lateral view; (L) paired dorsal processes in detail (indicated by square in K). Scale bars: 150 µm (A,); 100 µm (B, C, D, J, K); 200 µm (E, G); 25 µm (F); 20 µm (H, L); 150 µm (I)

Apices of the metathoracic legs extending beyond the base of abdominal segment A8. Thoracic segments (T1–T3) each bearing one pair of filiform setae in a dorsolateral position. Abdominal segments bearing numerous dorsal spinules (Fig. 6F), which are larger near the anterior margin of each segment. Segments A1–A7 each with three pairs of filiform setae, in dorsolateral, subdorsal, and lateral positions; the latter two pairs longer than the dorsolateral pair (Fig. 6E). Segment A8 additionally bearing a fourth filiform seta in a ventrolateral position (Fig. 6 J). Segment A9 with only one pair of setae in the dorsolateral position (Fig. 6I). Segment A10 (terminal abdominal segment) lacking filiform setae, but with two anteriorly directed, short, sharp dorsal processes (Fig. 6L) and a pair of divergent, long, sharp processes at the end (Fig. 6I). Abdominal segments A1–A8 each with a lobe or protuberance ("lateral callosities") located between the dorsolateral and lateral filiform setae, more conspicuous on segments A2–A4 (Fig. 6G). Spiracles with prespiracular setae located in an anterodorsal position (Fig. 6H).

Mandibular Ontogeny in Sap-Feeding Larvae and Leaf Damage (Fig. 7)

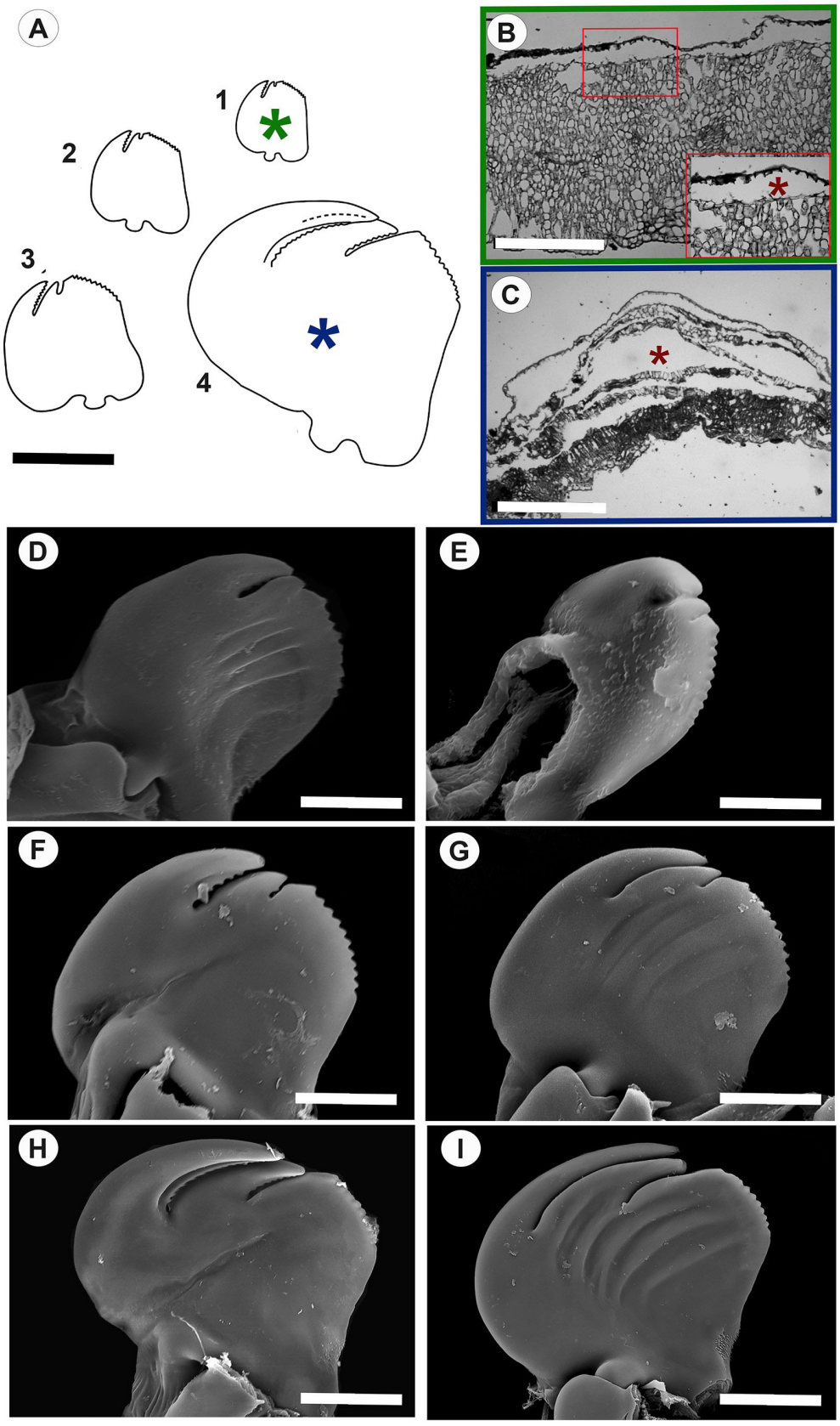

Figure 7 Mandibular morphology of *A. tecomae* sap-feeding instars and leaf damage on *Tecoma fulva*. In: (A) ontogenetic changes in mandibular morphology across sap-feeding instars (Arabic numerals indicate instars 1–4); (B) Transverse histological section of a mine produced by a first sap-feeding instar on *Tecoma fulva* (location indicated by line 1 in Fig. 1D); (C) Transverse histological section of a mine produced by a fourth sap-feeding instar on *Tecoma fulva* (location indicated by line 2 in Fig. 1D); (D–I) Scanning electron micrographs of mandibles of sap-feeding instars: (D) first instar, ventral view; (E) second instar, laterodorsal view; (F) third instar, dorsal view; (G) third instar, ventral view; (H) fourth instar, dorsal view; (I) fourth instar, ventral view. Scale bars: 25 µm (A, H, I); 300 µm (B); 400 µm (C); 5 µm (D); 10 µm (E); 15 µm (F, G). Red asterisks indicate larval mines; green asterisk indicate correspondence with Fig. 7B; blue asterisk indicate correspondence with Fig. 7C

The general morphology of the mandibles in sap-feeding larvae of *A. tecomae* is conserved across all four instars (as described above), with ontogenetic modifications detailed below. During the first three instars, the mandibles maintain their teeth aligned in a single plane without overlap (Fig. 7A, D-G), restricting the larvae to feeding on the epidermal layer of *Tecoma fulva* leaflets (Fig. 7B) and exhibiting a leaf-mining habit typical of serpentine mines (Fig. 1C, D), although these instars can also enter the parenchyma, albeit very superficially. In these instars, the mandibles increase in size from one instar to the next while retaining their overall shapes and the proportional spacing between the teeth and the mesial region; the second tooth is straight, short, and confined to the inner part of the mandible. By the third instar, the inner surface of the first tooth begins to show a slight serration in dorsal view (Fig. 7F). In the fourth instar, the position of the second tooth is slightly altered, becoming partially displaced beneath the first tooth, which extends marginally into an oval, sickle-like shape, thereby distinguishing it from the condition observed in earlier instars; the inner surface of the first tooth forms an invagination in the serrated region, while the second tooth develops a curved shape, extending to more than twice its previous length (Fig. 7H, I). This modification increases mandibular coverage and thickness, allowing the larvae to penetrate deeper into the leaf tissues, initially forming a darkened blotch (Fig. 1D) and facilitating the subsequent construction of the pupal chamber by the spinning larva, which consists of multiple layers of leaf tissue (Fig. 7C).

Discussion

The importance of conducting morphological descriptions supported by high-resolution visual tools, such as scanning electron microscopy, is particularly evident in immature stages of small-sized insects, such as microlepidopterans, for the accurate characterization and highlighting of morphological features that cannot be reliably observed using conventional techniques. Scanning electron microscopy has been widely applied in gracillariid leaf-mining moths to reveal fine structural details of larvae and pupae, facilitating comparative and taxonomic research (e.g. Brito et al., 2012; Kobayashi et al., 2013; Pereira et al., 2019; Cerdeña et al., 2020). In *A. tecomae*, the use of SEM allowed the documentation of structures not reported in the original description, such as pleural lobes on abdominal segment A9 and a fourth digitiform lobe on the antenna of the sap-feeding larva, as well as lateral callosities on pupal abdominal segments. Although the original description included some SEM images, these were limited in number and resolution, which may have constrained observation of finer morphological details. High-resolution imaging also allowed confirmation of the position of the sharp dorsal processes of abdominal segment A10 (cremaster) in the pupa, which were originally described as being located on segment A9 by Vargas and Parra (2005), and enabled the construction of a detailed chaetotaxic map for the larval stages, providing a more comprehensive framework for morphological comparisons in future studies.

Recent phylogenetic and taxonomic studies have emphasized the importance of immature-stage morphology in supporting higher-level relationships within Gracillariidae, particularly for the recognition of Oecophyllembiinae (Kumata, 1998; Kobayashi et al., 2013; Kawahara et al., 2017; Li et al., 2022). Characters related to larval feeding behavior, mandibular morphology, chaetotaxy, and pupal structures provide consistent diagnostic traits and complement molecular evidence (Kawahara et al., 2017). In the present study, the examination of the immature stages of *Angelabella tecomae* revealed several characters supporting its placement within Oecophyllembiinae, including the presence of larval spiracles on the mesothorax, pupal tergal spines bearing a single pair of dorsal setae, and a chaetotaxic pattern consistent with other oecophyllembiine genera. The pupa of *A. tecomae* also exhibits a cremaster with paired dorsal processes, a condition shared by all genera of the subfamily and considered informative for taxonomic identification (Kobayashi et al., 2011, 2013). However, the morphology of this structure appears to be unique in *A. tecomae* compared with other described genera, confirming its potential value as a diagnostic character at the generic level.

The larval chaetotaxic pattern of sap-feeding instars remains undescribed for most genera of Oecophyllembiinae, except for *Prophyllocnistis epidrymis* (Davis, 1994), in which six cranial setae (P1, P2, A1, A2, A3, and S) were reported. In contrast, nine cranial setae were identified in *A. tecomae* (A1, P1, P2, S1, S2, L1, SS1, SS2, and S3), with some apparent correspondence between the two species. However, differences in setal designation exist because the generalized lepidopteran setal pattern may be difficult to apply in the absence of stemmata as reference structures (as in *A. tecomae*) and the sap-feeding larval head is highly modified, with prognathous mouthparts, potentially leading to confusion in terminology (Davis, 1987). In addition, the absence of illustrations or a setal map of the head in sap-feeding instars of *P. epidrymis* prevents direct comparison. A comparative study is therefore needed to clarify setal homologies in sap-feeding instars to standardize terminology within the subfamily Oecophyllembiinae.

The spinning larva has been used to define diagnostic characters of Oecophyllembiinae (Kumata, 1998), including: absence of prothoracic and anal dorsal shields; thoracic spiracles opening in the anterolateral region of the mesothorax; presence of the MV group of proprioceptor setae (MV2 and MV3) on all thoracic segments; L-group setae on abdominal segments uni- or bisetose; SV-group setae on segments A2–A6 bisetose (SV1 and SV2), arranged in a vertical line anterior to ventral glabrous plates (reduced prolegs); and segment A9 bearing two or three pairs of tactile setae. The present study confirms that *A. tecomae* exhibits these characters, with some differences; the "MV group" *sensu* Kumata (1998) is here interpreted as the SV group, therefore we propose treating this setal group as SV. In addition, the SV group in *A. tecomae* is trisetose on abdominal segments A3–A6 and bisetose on A2, while maintaining the characteristic vertical arrangement anterior to ambulatory callosities.

Several studies on leaf-mining insects indicate that feeding patterns and the depth of tissue consumption are strongly influenced by the distribution of nutritional quality and structural defenses within the leaf (Scriber and Slansky Junior, 1981; Ayabe, 2010). Mining larvae often preferentially exploit nutrient-rich mesophyll tissues while avoiding structurally reinforced or nutritionally poorer layers such as the epidermis and vascular tissues (Kimmerer and Potter, 1987; Giron et al., 2016; Tooker and Giron, 2020). In Gracillariidae, this pattern is closely associated with ontogenetic shifts in feeding mode, with early instars acting as sap-feeders and later instars consuming and disrupting mesophyll tissues more extensively to exploit internal leaf resources, highlighting the importance of internal leaf tissues as a nutritional resource during development (Body et al., 2015; Guiguet et al., 2018). However, in *A. tecomae*, the deeper exploitation of mesophyll tissue may be more closely related to an initial structural or protective function associated with pupal chamber construction rather than to nutritional requirements alone, as the fourth-instar larva remains restricted to the zone where the pupal chamber will later be constructed, without expanding its mine across the leaflet—where additional feeding could occur—and retains a sap-feeding condition without transitioning to tissue-feeding, suggesting a reduced selective pressure for continued feeding. This interpretation is further supported by the ontogenetic modification of the mandibles described here, which enables the addition of multiple layers through deeper tissue penetration, thereby potentially enhancing protection under the xeric environmental conditions in which the species occurs, likely as a result of environmental selective pressures for tolerance of desiccation (Connor and Taverner, 1997).

This hypothesis remains to be tested in future studies, particularly within the subfamilies Oecophyllembiinae, Phyllocnistinae, and Marmarinae, in which several sap-feeding instars are followed by one or two spinning instars prior to pupation, or through comparative analyses of species inhabiting xeric environments.

Acknowledgments

Thanks are due to Luis Figueroa (Departamento de Entomología, MUSM) and Danayra Cruz (Laboratorio de Equipamiento Especializado, UNMSM) for assistance and use of scanning electron microscopy facilities. Our thanks also go to the reviewers of the document for their valuable comments.

Funding

This work was supported by the Consejo Nacional de Ciencia, Tecnología e Innovación (CONCYTEC) and the Programa Nacional de Investigación Científica y Estudios Avanzados (PROCIENCIA) through the Call E077-2023-01-BM "Becas en Programas de Doctorado en Alianzas Interinstitucionales" (PE5010 88688-2024) and through the Call E033-2023-01-BM "Alianzas Interinstitucionales para Programas de Doctorado" (PE501085130-2023).

Data statement

The entire dataset supporting the results of this study was published in the article itself.

Conflicts of interest

The authors declare no conflict of interest.

Author contribution statement

JC Conceptualization, methodology, writing - original draft, writing - review and editing, funding acquisition. JF Conceptualization, methodology, writing - review and editing. HAV Conceptualization, methodology, writing - review and editing, supervision. GL Conceptualization, writing - review and editing, supervision.

References

Álvarez, Y., Núñez, R., Magaldi, L. D. M., Matthews, D., Freitas, A. V. L., Espeland, M., 2025. Phenotypes, natural history and barcodes unveil cryptic species within the Caribbean Metalmark *Dianesia carteri* (Holland) (Lepidoptera: riodinidae). Zootaxa 5686 (1), 5-48. https://doi.org/10.11646/zootaxa.5686.1.2.

Ayabe, Y., 2010. Specific mining pattern as a result of selective feeding within a leaf by the dipteran leafminer *Ophiomyia maura.* Ann. Entomol. Soc. Am. 103 (5), 806-812. https://doi.org/10.1603/AN10049.

Body, M., Burlat, V., Giron, D., 2015. Hypermetamorphosis in a leaf-miner allows insects to cope with a confined nutritional space. Arthropod-Plant Interact. 9 (1), 75-84. https://doi.org/10.1007/s11829-014-9349-5.

Brito, R., Gonçalves, G. L., Vargas, H. A., Moreira, G. R. P., 2012. A new species of *Phyllocnistis* Zeller (Lepidoptera: Gracillariidae) from southern Brazil, with life-history description and genetic comparison to congeneric species. Zootaxa 3582 (1), 1-16. https://doi.org/10.11646/zootaxa.3582.1.1.

Cerdeña, J., Farfán, J., Vargas, H. A., Brito, R., Gonçalves, G. L., Lazo, A., Moreira, G. R. P., 2020. *Phyllocnistis furcata* sp. nov.: a new species of leaf-miner associated with *Baccharis* (Asteraceae) from Southern Peru (Lepidoptera, Gracillariidae). ZooKeys 996, 121-145. https://doi.org/10.3897/zookeys.996.53958.

Connor, E. F., Taverner, M. P., 1997. The evolution and adaptive significance of the leaf-mining habit. Oikos 79 (1), 6-325. https://doi.org/10.2307/3546085.

Davis, D. R., 1987. Gracillariidae. In: Stehr, F.W. (Ed.), Immature Insects. Vol. 1. Kendall/Hunt Publishing Company, Dubuque, pp. 372-374.

Davis, D. R., 1994. New leaf-mining moths from Chile, with remarks on the history and composition of Phyllocnistinae (Lepidoptera: gracillariidae). Trop. Lepid. 5 (1), 65-75.

Davis, D. R., Wagner, D. L., 2011. Biology and systematics of the New World *Phyllocnistis* Zeller leafminers of the avocado genus *Persea* (Lepidoptera, Gracillariidae). ZooKeys 97, 39-73. https://doi.org/10.3897/zookeys.97.753.

Friberg, M., 2007. A difference in pupal morphology between the sibling species *Leptidea sinapis* and *L. reali* (Pieridae). Nota Lepidopterol. 30 (1), 61-64.

Garzón-Orduña, I. J., Brower, A. V. Z., 2025. A new cryptic *Phyllodonta* Warren (Lepidoptera: Geometridae) from Mexico City with documentation of its life history. Zootaxa 5666 (1), 136-144. https://doi.org/10.11646/zootaxa.5666.1.8.

Giron, D., Huguet, E., Stone, G. N., Body, M., 2016. Insect-induced effects on plants and possible effectors used by galling and leaf-mining insects to manipulate their host-plant. J. Insect Physiol. 84, 70-89. https://doi.org/10.1016/j.jinsphys.2015.12.009.

Guiguet, A., Hamatani, A., Amano, T., Takeda, S., Lopez-Vaamonde, C., Giron, D., Ohshima, I., 2018. Inside the horn of plenty: leaf-mining micromoth manipulates its host plant to obtain unending food provisioning. PLoS One 13 (12), e0209485. https://doi.org/10.1371/journal.pone.0209485.

Kawahara, A. Y., Plotkin, D., Ohshima, I., Lopez-Vaamonde, C., Houlihan, P. R., Breinholt, J. W., Kawakita, A., Xiao, L., Regier, J. C., Davis, D. R., Kumata, T., Sohn, J.-C., De Prins, J., Mitter, C., 2017. A molecular phylogeny and revised higher-level classification for the leafmining moth family Gracillariidae and its implications for larval host-use evolution. Syst. Entomol. 42 (1), 60-81. https://doi.org/10.1111/syen.12210.

Kimmerer, T. W., Potter, D. A., 1987. Nutritional quality of specific leaf tissues and selective feeding by a specialist leafminer. Oecologia 71 (4), 548-551. https://doi.org/10.1007/BF00379295.

Kobayashi, S., Huang, G.-H., Hirowatari, T., 2011. Two species of Gracillariidae (Lepidoptera) new to China, and description of the pupal morphology of the genera *Corythoxestis* and *Eumetriochroa.* Zootaxa 2892 (1), 25-32. https://doi.org/10.11646/zootaxa.2892.1.2.

Kobayashi, S., Huang, G.-H., Nakamura, A., Hirowatari, T., 2013. Four new species of Gracillariidae (Lepidoptera) from China and Japan, and description of the pupal morphology of the genera *Corythoxestis, Eumetriochroa, Guttigera*, and *Metriochroa.* Zootaxa 3619 (2), 101-129. https://doi.org/10.11646/zootaxa.3619.2.1.

Kumata, T., 1978. A new stem-miner of alder in Japan with a review of the larval transformation in the Gracillariidae (Lepidoptera). Insecta Matsumurana 13, 1-27.

Kumata, T., 1998. Japanese species of the subfamily Oecophyllembiinae Réal et Balachowsky (Lepidoptera: Gracillariidae), with description of a new genus and eight new species. Insecta Matsumurana 54, 77-131.

Li, X., St Laurent, R., Earl, C., Doorenweerd, C., van Nieukerken, E. J., Davis, D. R., Johns, C. A., Kawakita, A., Kobayashi, S., Zwick, A., Lopez-Vaamonde, C., Ohshima, I., Kawahara, A. Y., 2022. Phylogeny of gracillariid leaf-mining moths: evolution of larval behaviour inferred from phylogenomic and Sanger data. Cladistics 38 (3), 277-300. https://doi.org/10.1111/cla.12490.

Pereira, C. M., Arévalo-Maldonado, H. A., Triberti, P., Brito, R., Isaias, R. M. S., Gonçalves, G. L., Moreira, G. R. P., 2019. *Vallissiana universitaria* (Lepidoptera, Gracillariidae): a new genus and species of leaf-mining moth associated with *Erythroxylum* (Erythroxylaceae) in the Atlantic Forest of Brazil. Zootaxa 4604 (1), 141-160. https://doi.org/10.11646/zootaxa.4604.1.5.

Scriber, J. M., Slansky Junior, F., 1981. The nutritional ecology of immature insects. Annu. Rev. Entomol. 26 (1), 183-211. https://doi.org/10.1146/annurev.en.26.010181.001151.

Storey-Palma, J., Benítez, H., Parra, L. E., Vargas, H. A., 2012. Identification of sap-feeder instars in *Angelabella tecomae* Vargas & Parra (Lepidoptera, Gracillariidae) feeding on *Tecoma fulva fulva* (Bignoniaceae). Rev. Bras. Entomol. 56 (4), 508-510. https://doi.org/10.1590/S0085-56262012000400018.

Tooker, J. F., Giron, D., 2020. The evolution of endophagy in herbivorous insects. Front. Plant Sci. 11, 581816. https://doi.org/10.3389/fpls.2020.581816.

Vargas, H. A., Parra, L. E., 2005. Un nuevo género y una nueva especie de Oecophyllembiinae (Lepidoptera: Gracillariidae) de Chile. Neotrop. Entomol. 34 (2), 227-233. https://doi.org/10.1590/S1519-566X2005000200011.

Vargas-Ortiz, M., Aliaga-Pichihua, G., Lazo-Rivera, A., Cerdeña, J., Farfán, J., Huanca-Mamani, W., Vargas, H. A., 2020. Cryptic diversity in the monotypic Neotropical micromoth genus *Angelabella* (Lepidoptera: Gracillariidae) in the Peru-Chile desert. Insects 11 (10), 677. https://doi.org/10.3390/insects11100677.